TOXICOLOGICAL SCIENCES **133(1)**, 90–100 2013
doi:10.1093/toxsci/kft022
Advance Access publication February 1, 2013

Decreased Zinc Availability Affects Glutathione Metabolism in Neuronal Cells and in the Developing Brain

Yo Omata,*[,1] Gabriela A. Salvador,†[,1] Suangsuda Supasai,* Alison H. Keenan,* and Patricia I. Oteiza*[,2]

*Department of Nutrition and Department of Environmental Toxicology, University of California, Davis, California 95616; and †Instituto de Investigaciones Bioquímicas de Bahía Blanca, Universidad Nacional del Sur and Consejo Nacional de Investigaciones Científicas y Técnicas (CONICET), Bahía Blanca, Buenos Aires, Argentina

[1]These authors contributed equally to this work.
[2]To whom correspondence should be addressed at Department of Nutrition, University of California, Davis One Shields Av., Davis, CA 95616. Fax: (530) 752-8966. E-mail: poteiza@ucdavis.edu.

Received December 13, 2012; accepted January 15, 2013

A deficit in zinc (Zn) availability can increase cell oxidant production, affect the antioxidant defense system, and trigger oxidant-sensitive signals in neuronal cells. This work tested the hypothesis that a decreased Zn availability can affect glutathione (GSH) metabolism in the developing rat brain and in neuronal cells in culture, as well as the capacity of human neuroblastoma IMR-32 cells to upregulate GSH when challenged with dopamine (DA). GSH levels were low in the brain of gestation day 19 (GD19) fetuses from dams fed marginal Zn diets throughout gestation and in Zn-deficient IMR-32 cells. γ-Glutamylcysteine synthetase (GCL), the first enzyme in the GSH synthetic pathway, was altered by Zn deficiency (ZD). The protein and mRNA levels of the GCL modifier (GCLM) and catalytic (GCLC) subunits were lower in the Zn-deficient GD19 fetal brain and in IMR-32 cells compared with controls. The nuclear translocation of transcription factor nuclear factor (erythroid-derived 2)-like 2, which controls GCL transcription, was impaired by ZD. Posttranslationally, the caspase-3-dependent GCLC cleavage was high in Zn-deficient IMR-32 cells. Cells challenged with DA showed an increase in GCLM and GCLC protein and mRNA levels and a consequent increase in GSH concentration. Although Zn-deficient cells partially upregulated GCL subunits after exposure to DA, GSH content remained low. In summary, results show that a low Zn availability affects the GSH synthetic pathway in neuronal cells and fetal brain both at transcriptional and posttranslational levels. This can in part underlie the GSH depletion associated with ZD and the high sensitivity of Zn-deficient neurons to pro-oxidative stressors.

Key Words: **zinc; zinc deficiency; Nrf2; glutathione; dopamine; neuron; γ-glutamylcysteine synthetase**

Zinc (Zn) is an essential nutrient with multiple roles in the nervous system (Frederickson *et al.*, 2005). Deficits of this nutrient during early development result in adverse effects on brain structure and function (Uriu-Adams and Keen, 2010). Dietary Zn deficiency (ZD) affects the central nervous system resulting in altered behavior, learning, and memory (Bentley *et al.*, 1997; Gardner *et al.*, 2005; Penland *et al.*, 1997). Given the requirement of Zn for numerous cell processes, the above alterations are probably multifactorial. A consistent finding when neuronal Zn decreases is a condition of oxidative stress (Mackenzie *et al.*, 2006b; Oteiza and Mackenzie, 2005), which can be accompanied by alterations in cell thiol redox status. In this regard, decreased Zn availability causes tubulin thiol oxidation, impairing tubulin dynamics and function, both in neuronal cells and in the developing brain (Mackenzie *et al.*, 2011). ZD is also consistently associated with decreased levels of glutathione (GSH) and oxidative stress in different cells and tissues (El-Seweidy *et al.*, 2008; Kojima-Yuasa *et al.*, 2005; Kraus *et al.*, 1997; Mackenzie *et al.*, 2006a; Tomat *et al.*, 2008). GSH is the most abundant nonprotein thiol synthesized in cells and a central component of the antioxidant defense system. In IMR-32 neuroblastoma cells, ZD leads not only to protein thiol oxidation but to a decrease in GSH levels, which is prevented by Zn supplementation (Mackenzie *et al.*, 2006b).

GSH is central in the metabolism of H_2O_2 and lipid peroxides, can react with carbon-centered radicals, and participates in the detoxification of xenobiotics through conjugation reactions (Forman *et al.*, 2009). Furthermore, through its key role in the maintenance of an optimal intracellular redox environment, GSH is part of numerous basic cellular processes including the regulation of redox signaling, protein and DNA synthesis, DNA repair, cell proliferation, and programmed cell death (Circu and Aw, 2010; Jones, 2008). GSH is absolutely essential for mammalian life as evidenced by the embryonic lethality observed in glutamate cysteine ligase (GCL) knock-out mice (Dalton *et al.*, 2000). The synthesis of GSH, a tripeptide (γ-glutamylcysteinylglycine), from its constituent amino acids is both constitutive and regulated. GSH is synthesized through the concerted action of two enzymes, GCL and GSH synthase. GCL catalyzes the formation

of γ-glutamylcysteine, the rate-limiting step for *de novo* GSH synthesis. GCL consists of a catalytic subunit (GCLC, 73 kDa), which contributes to all the enzymatic activity containing the substrate binding sites. The GCL modifier subunit (GCLM, 31 kDa) modulates the affinity of GCLC for substrates and inhibitors. GCL belongs to the group of phase II detoxification enzymes and its expression is regulated by transcription factor nuclear factor (erythroid-derived 2)-like 2 (Nrf2) (Hansen *et al.*, 2004). The expression of both GCL subunits is induced in response to various agents, including oxidative stressors. The inducible nature of GCL makes it a crucial component of the cellular adaptation machinery for resistance against oxidative stress (Circu and Aw, 2010; Forman *et al.*, 2009).

ZD not only can cause oxidative stress but also increases the susceptibility of neurons to pro-oxidant stressors, including lead and iron (Aimo and Oteiza, 2006; Mackenzie *et al.*, 2002a). Extensive evidence supports a role for dopamine (DA)-mediated oxidative stress in the neurotoxicity associated with the development of neurodegenerative processes (e.g., Parkinson's disease [PD]). DA is a neurotransmitter that can undergo oxidation to form quinone and semiquinone derivatives that are highly reactive toward sulfhydryl groups. The thiol-containing compounds GSH, cysteine, and N-acetyl cysteine prevent DA autoxidation *in vitro* and decrease the size of damaged area in rat striatum when coinjected with DA (Soto-Otero *et al.*, 2000). Survival of dopaminergic neurons crucially depends on a tight regulation of their GSH levels, being GSH synthesis upregulated upon DA exposure (Jia *et al.*, 2008). GSH deficits have been found in the brain of PD and schizophrenic patients, which could constitute a causative insult triggering neuronal degeneration (Garrido *et al.*, 2011; Gysin *et al.*, 2007). On the other hand, the mobilization of Zn from metallothionein, as a consequence of DA-mediated metallothionein thiol oxidation, has been proposed as a protective neuronal response against DA-induced oxidative damage (Eibl *et al.*, 2010). Furthermore, ZD-induced epigenetic alterations in the metal responsive elements within the promoter region of the metallothionein gene (Kurita *et al.*, 2013) could be also involved in an increased susceptibility to oxidative stressors (e.g., DA).

We propose that ZD-induced neuronal oxidative stress and the increased susceptibility of Zn-deficient neuronal cells to oxidative stressors could be in part due to an impaired GSH synthesis when neuronal Zn decreases. To test this hypothesis, the effects of ZD on the regulation of GCL expression and GSH levels were investigated in fetal rat brain and in human IMR-32 neuroblastoma cells. The capacity of Zn-deficient neuronal cells to upregulate GCL in response to DA-mediated neuronal injury was also studied.

MATERIALS AND METHODS

Materials. IMR-32 cells were from the American Type Culture Collection (Rockville, MA). Cell culture media, reagents, SuperScript III First-Strand Synthesis System, and LipofectAMINE 2000 were from Invitrogen Life Technologies (Carlsbad, CA). The antibodies for β-tubulin (SC-9104), GCLC (SC-22755), GCLM (SC-22754), and PARP (SC-7150) were from Santa Cruz Biotechnology (Santa Cruz, CA). PVDF membranes were from Bio-Rad (Hercules, CA). The ECL plus Western blotting system was from Amersham Pharmacia Biotech Inc. (Piscataway, NJ). The ApoAlert-Caspase-3 Assay was from Promega (Madison, WI). The RNeasy Mini Kit Isolation System and QIA shredder were from Qiagen Ltd (Valencia, CA). The caspase-3 inhibitor Ac-VEID-CHO was purchased from Calbiochem (Merck KGaA, Darmstadt, Germany). DA and all other reagents were from the highest quality available and were purchased from Sigma-Aldrich Co. (St Louis, MO).

Animal studies. All procedures were in agreement with standards for the care of laboratory animals as outlined in the National Institutes of Health Guide for the Care and Use of Laboratory Animals. All procedures were administered under the auspices of the Animal Resource Services of the University of California, Davis, which is accredited by the American Association for the Accreditation of Laboratory Animal Care. Experimental protocols were approved before implementation by the University of California, Davis, Animal Use and Care Administrative Advisory Committee and were administered through the Office of the Campus Veterinarian. Adult Sprague Dawley rats (Charles River, Wilmington, MA) (200–225 g) were housed individually in suspended stainless steel cages in a temperature (22°C–23°C)- and photoperiod (12 h light/dark)-controlled room. An egg white protein–based diet with adequate Zn (25 μg Zn/g) was the standard control diet (Keen *et al.*, 1989). Animals were fed the control diet for 1 week before breeding. Males and females were caged together overnight and the following morning, the presence of a sperm plug confirmed a successful breeding. On gestation day (GD) 0, rats (nine animals per group) were divided into two groups and fed *ad libitum* a control diet (25 μg Zn/g diet) or a diet containing a marginal concentration of Zn (10 μg Zn/g diet, marginal Zn [MZ]) until GD19. Food intake was recorded daily, and body weight was measured at 5-day intervals. Food intake and body weight gain throughout gestation were similar in both groups. At GD19, dams were anesthetized with isofluorane (2 mg/kg body weight), and laparotomies were performed. The gravid uterus was removed, and fetuses collected. Fetal brains were excised, rinsed in ice-cold PBS, the meninges removed, weighed and processed for GSH determination (three brains per litter), Western blot, and real-time PCR (RT-PCR) (one brain per litter). This experimental model in rats is considered as a condition of MZ nutrition because it affords normal pregnancy and fetal outcomes, whereas ZD causes profound effects on pregnancy outcome and teratogenicity (Aimo *et al.*, 2010b).

Cell cultures. Zn-deficient fetal bovine serum (FBS) was prepared by chelation with diethylenetriaminepentaacetic acid as previously described (Duffy *et al.*, 2001; Oteiza *et al.*, 2000). The chelated FBS was subsequently diluted with complex medium (55% [vol/vol] Dulbecco's Modified Eagle's Medium high glucose [HyClone SH30022.01], 30% [vol/vol] Ham F-12 [HyClone SH30026.01], 5% [vol/vol] α-Minimum Essential Medium [HyClone SH30054.02]) to a final concentration of 3 mg protein/ml to match the protein concentration of the control nonchelated medium (10% [vol/vol] FBS). Zn, copper, and iron concentrations were determined for each batch of chelated serum by inductively coupled plasma-atomic emission spectroscopy analysis (Trace Scan, Thermo Jarrell Ash Corp., Franklin, MA). As previously described (Oteiza *et al.*, 2000), concentrations for copper and iron were fixed at 1 and 5μM concentrations, respectively, to eliminate these cations as potential variables. The concentration of Zn in the control and deficient media was 6 and 1.5μM, respectively.

IMR-32 cells were cultured at 37°C in complex medium supplemented with 10% (vol/vol) FBS and antibiotic-antimycotic (50 U/ml penicillin, 50 μg/ml streptomycin, and 0.125 μg/ml amphotericin B). Cells were grown in complex medium containing 10% (vol/vol) nonchelated FBS until 90% confluence. IMR-32 cells were subsequently incubated in control nonchelated medium or in chelated media containing 1.5μM Zn. In some experiments, 50μM DA was added and cells were harvested after 6–24 h in culture.

GSH determination. GSH determination in fetal brain and IMR-32 cells was done as described by Jones *et al.* (1998). Briefly, brain samples or cells

were immediately homogenized in PBS containing 0.1% (vol/vol) Igepal. After separating an aliquot for subsequent protein determination, samples (150 µl) were added with 100 µl of perchloric acid (10% [wt/vol]) and centrifuged. The supernatant was decanted, and 150 µl aliquots were added with 30 µl iodoacetic acid (40mM) and 140 µl KOH (1M)/tetrahydroborate (2.3M) to adjust the pH to 9. Subsequently, 150 µl of a 20 mg dansyl chloride/ml acetone solution was added. Derivatization was carried out in the dark for 16 h at room temperature and the excess of dansyl chloride was extracted with 250 µl of chloroform. For GSH and oxidized GSH (GSSG) determinations by high-performance liquid chromatography, a 3-aminopropyl column was used. The mobile phase was formed by a gradient with two solvent systems (80% [vol/vol] methanol/water and acetate-buffered methanol, pH 4.6) that were mixed as described (Jones *et al.*, 1998). Fluorescent detection of GSH was done at λexc: 395 nm and λem: 510–650 nm.

Western blot analysis. For the preparation of total or nuclear cell extracts, cells (20×10^6 cells) were rinsed with PBS, scrapped, and centrifuged. The pellet was rinsed with PBS and suspended in 200 µl of 50 mmol/l HEPES (pH 7.4), 125mM KCl containing protease inhibitors, and 2% (vol/vol) Igepal. The final concentration of the inhibitors was 0.5 mmol/l PMSF, 1 mg/l leupeptin, 1 mg/l pepstatin, 1.5 mg/l aprotinin, 2 mg/l bestatin, and 0.4mM sodium pervanadate. Samples were exposed to one cycle of freezing and thawing, incubated at 4°C for 30 min, and centrifuged at 15,000 × g for 30 min. The supernatant was decanted and protein concentration was measured.

Aliquots of total cell extracts containing 25–50 µg protein were separated by reducing 10% (wt/vol) polyacrylamide gel electrophoresis and electroblotted to PVDF membranes. Colored molecular weight standards (Amersham Pharmacia Biotech Inc.) were ran simultaneously. Membranes were blotted for 2 h in 5% (wt/vol) nonfat milk and incubated overnight in the presence of corresponding primary antibodies (1:1000–1:2000 dilution) at 4°C. After incubation for 90 min at room temperature in the presence of the secondary antibody (horseradish peroxidase conjugated) (1:10,000 dilution), the conjugates were visualized by chemiluminescence detection in a Phosphorimager 840.

Determination of mRNA levels. Total RNA was extracted from fetal brain and cells using an optimized RNA extraction protocol based on the RNeasy Mini Kit Isolation System (Qiagen Ltd) according to the manufacturer's protocol. Cells were grown in 6-well plates, and after the corresponding treatments resuspended in 350 µl of lysis buffer and homogenized using QIA shredder (Qiagen Ltd) at 8000 g for 2 min. The RNA was eluted using 50 µl of nuclease-free water and stored at −80°C until use. cDNA was synthesized using the SuperScript III First-Strand Synthesis System for RT-PCR (Invitrogen) according to the manufacturer's protocol. Samples were stored at −80°C.

The expression of GCLC and GCLM mRNA was determined by RT-PCR using the following primers: for rat GCLC: 5′-GGGAAGGAAGGCGT GTTTCCT-3′ (forward) and 5′-GTCGACTTCCATGTTTTCAAGGT-3′ (reverse); for rat GCLM: 5′-CCAGGAGTG GGTGCCACTGT-3′ (forward) and 5′-TTTGACTTGATGATTCCTCTGCTT-3′ (reverse); for human GCLC: 5′-GGCTGAGTGTCCGTCTCG-3′ (forward) and 5′- GTGGTAGA TGTGCAGGAACT-3′ (reverse); for human GCLM: 5′-GCCCTTTA AAGA GACGTGTAGGAA-3′ (forward) and 5′-CCGCCTGGTGAGGTAGAC-3′ (reverse). RT-PCR was conducted using iQ iCycler Detection System (Bio-Rad Laboratories, Ltd), and PCR amplification was then detected with the SYBR green fluorophore. A control cDNA dilution series was created for the gene to establish a standard curve. Each reaction was subjected to melting point analysis to confirm single amplified products. The data generated from each PCR were analyzed using iQ iCycler Optical System Software Version 3.0a (Bio-Rad Laboratories, Ltd). The housekeeping gene *RiboL32* was used as an endogenous control. The primers for the amplification of human *RiboL32* were as follows: 5′-GAAACTCGCGGAAACCCA-3′ (forward) and 5′-GGATCTGGCCCTTGAACCTTC-3′ (reverse); and for rat *RiboL32*: 5′-GAAACTCGCGGAAACCCA-3′ (forward) and 5′-AGATCTGGCCCTTGAATCTTC -3′ (reverse).

Assay of GCL activity. GCL activity was measured in IMR-32 cell–soluble fractions using the 96-well microtiter plate method described by White *et al.* (2003), with minor modifications (Gupta *et al.*, 2012). Briefly, IMR-32 cells were homogenized in 20mM Tris-Cl buffer, pH 7.4, containing 250mM sucrose, 1mM EDTA, 20mM sodium borate, and 2mM serine. Homogenates were centrifuged at 12,000 × g for 10 min at 4°C, and the supernatants were decanted. Supernatant aliquots (50 µl, 4 µg protein/µl) were transferred to a 96-well plate, added with 50 µl 400mM Tris buffer, pH 7.4, containing 40mM ATP, 20mM L-glutamic acid, 2.0mM EDTA, 20mM sodium borate, 2mM serine, and 40mM $MgCl_2$ and incubated for 10 min at 37°C. The reaction was initiated by adding 50 µl 5mM L-cysteine. After incubating for 15 min at 37°C, the reaction was stopped by adding 50 µl of ice-cold 200mM sulphosalicylic acid, and samples incubated on ice for 20 min. The plate was subsequently centrifuged at 500 × g for 20 min, and 20 µl of samples and standards were transferred to a 96-well black plate. Samples and standards were derivatized under low light by adding 180 µl of naphthalene dicarboxaldehyde alkaline solution (140 µl 50mM Tris-base, pH 10, 20 µl 1M NaOH, and 20 µl 10mM naphthalene dicarboxaldehyde in dimethyl sulfoxide) for 30 min. The fluorescence ratio of γ-glutamylcysteine/GSH was measured at λexc: 427 nm and λem: 528 nm.

Electrophoretic mobility shift assay. Nuclear fractions were isolated as previously described (Osborn *et al.*, 1989), with minor modifications (Mackenzie *et al.*, 2002b). Protein concentration was measured as described by Bradford (1976). For the electrophoretic mobility shift assay (EMSA), the oligonucleotide containing the antioxidant response element (ARE) consensus sequence (5′-GGA ATT CTG TTT TCG CTG TCA TGG TTC-3′) (Operon, Huntsville, AL) (Banning and Brigelius-Flohé, 2005) was end-labeled with [$^{\gamma\text{-}32}$P] ATP using T4 polynucleotide kinase and purified using Chroma Spin-10 columns. Samples were incubated with the labeled oligonucleotide (20,000–30,000 cpm) for 20 min at room temperature in 1× binding buffer (5× binding buffer: 50mM Tris-HCl buffer, pH 7.5, containing 20% [vol/vol] glycerol, 5mM $MgCl_2$, 2.5mM EDTA, 2.5mM DTT, 250mM NaCl, and 0.25 mg/ml poly(dI-dC)). The products were separated by electrophoresis in a 6% (wt/vol) nondenaturing polyacrylamide gel using 0.5× TBE (Tris/borate 45mM, EDTA 1mM) as the running buffer. The gels were dried and the radioactivity quantified in a Phosphorimager 840 (Amersham Pharmacia Biotech Inc.).

Assay of caspase-3 activity. Caspase-3 activity was determined in cell lysates after incubating IMR-32 cells for 6 or 24 h in control or chelated media containing 1.5µM Zn in the absence or in the presence of DA (50µM). Caspase-3 activity was measured using the ApoAlert-Caspase-3 Assay following the manufacturer's protocol.

Statistical analysis. One-way ANOVA with subsequent *post hoc* comparisons by Scheffe was performed using Statview 5.0.1 (Brainpower Inc., Calabasas, CA). A p value < 0.05 was considered statistically significant. Values are given as means ± SEM.

RESULTS

ZD Diminishes GSH, GCL Protein, and mRNA Levels in Rat Fetal Brain

We previously observed that feeding rats MZ diets throughout gestation causes a decrease in Zn concentration and increased tubulin thiol oxidation in the brain of GD19 fetuses (Bentley *et al.*, 1997). We now investigated in the same experimental model if gestational MZ nutrition could affect GD19 fetal brain GSH and GCL levels. In MZ fetal brains, GSH content was significantly lower (21%) compared with controls (Fig. 1A). To evaluate if the decrease in GSH content could be associated with an impaired GSH *de novo* synthesis, the expression of GCL subunits was assessed measuring protein levels by immunoblotting and mRNA levels by RT-PCR. GD19 fetal brain GCLC and GCLM protein levels were 25

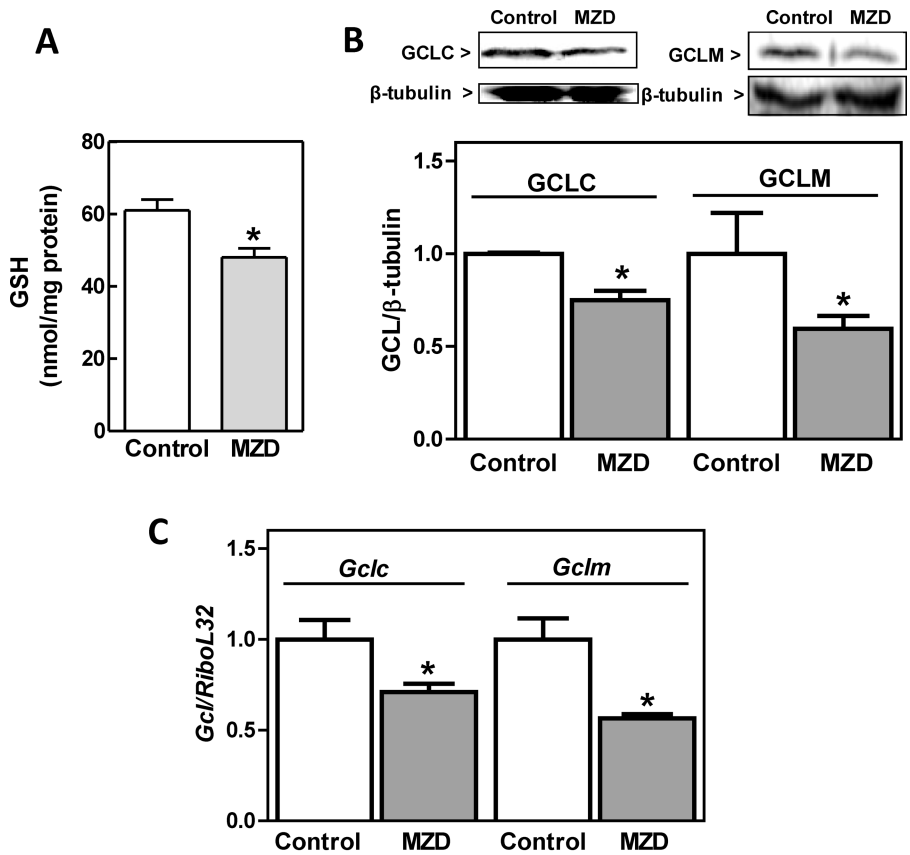

FIG. 1. ZD decreased GSH content and GCL expression in rat fetal brain. Rat dams were fed control or MZ diets (MZD) from GD0 until GD19. Fetal brains were excised and processed for the different determinations as described in the Materials and Methods section. (A) GSH concentration in 100,000 × g supernatants from MZ and control GD19 fetal brain were determined by HPLC. (B) Fetal brain GCLC, GCLM, and β-tubulin content were measured in total homogenates by Western blot. One representative image is shown. After quantification, results were expressed as the ratio of GCLC or GCLM/β-tubulin. C-GCLC and GCLM mRNA levels were measured by RT-PCR and values normalized to those of the ribosomal protein L32 (RPL32). Results are shown as means ± SEM. For GSH determination, three brains from each litter were pooled and results are means of nine litters per group; for RT-PCR and Western blot, results are means of one fetal brain per litter from six litters per group. *Significantly different compared with the control group ($p < 0.05$, one-way ANOVA test).

and 40% lower, respectively, in the MZ group compared with controls (Fig. 1B). Accordingly, the mRNA levels of *Gclc* and *Gclm* subunits were 29 and 44% lower in MZ fetal brains than in controls (Fig. 1C).

ZD Diminishes GCL Protein and mRNA Levels in IMR-32 Cells

We next examined the expression of GCL subunits in a model of neuronal ZD. Human neuroblastoma IMR-32 cells were incubated for 24 h in control or Zn-deficient (1.5μM Zn) medium. We previously showed that under similar experimental conditions, ZD increases IMR-32 cell oxidant levels and decreases GSH levels (Mackenzie *et al.*, 2006b), and labile (Mackenzie *et al.*, 2002b) and total Zn content (Mackenzie *et al.*, 2011). GSH decrease in IMR-32 incubated in Zn-deficient medium was prevented by supplementing the medium with Zn (15μM final concentration) (Mackenzie *et al.*, 2006b). GCLC and GCLM protein levels were 26 and 31% lower, respectively, after 24 h incubation in Zn-deficient media than in controls (Fig. 2A). mRNA levels measured by RT-PCR showed a lower expression of *Gclc* and *Gclm* subunits (31 and 33%, respectively) in Zn-deficient IMR-32 cells compared with controls (Fig. 2B). GCL activity was 44% lower in cells incubated in Zn-deficient medium for 24 h than in controls (Fig. 2C).

ZD Impairs Nrf2-DNA Binding in Rat Fetal Brain and IMR-32 Cells

GCL belongs to the group of phase II detoxification enzymes and its expression is in part regulated through the ARE by transcription factor Nrf2 (Hansen *et al.*, 2004). We next investigated whether the decreased GCL expression in Zn-deficient fetal brain and IMR-32 cells occurs as a consequence of an impaired Nrf2 transcriptional activity. For this purpose, we evaluated Nrf2-DNA binding by EMSA in nuclear fractions. Nrf2-DNA binding was 35% lower in nuclear fractions isolated from MZ rat fetal brains compared with controls (Fig. 3). Nrf2-DNA binding in nuclear fractions isolated from IMR-32 cells incubated for 24 h in Zn-deficient

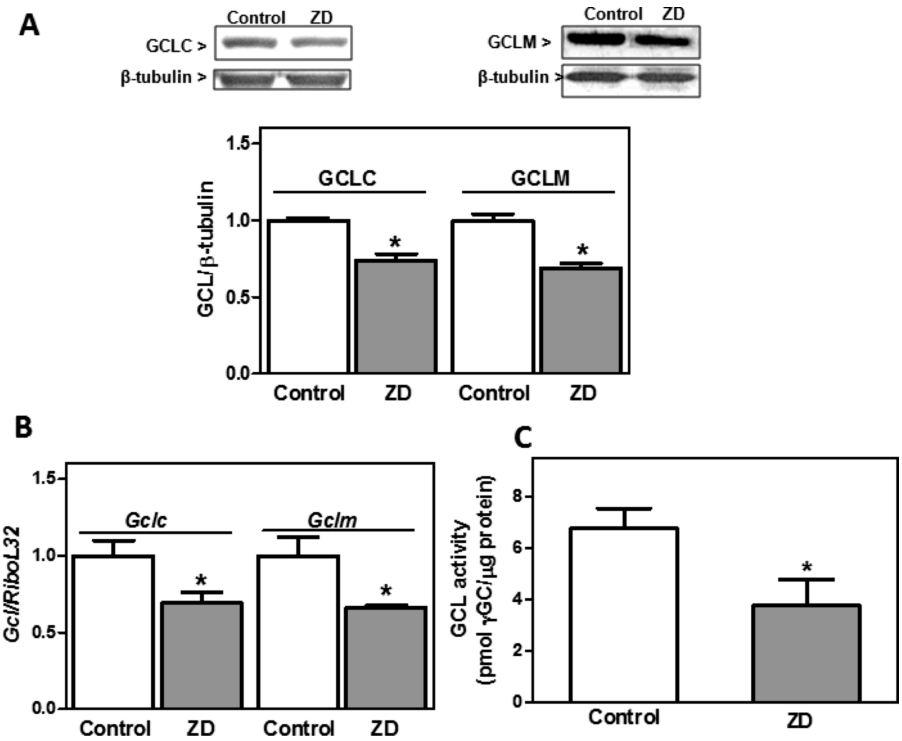

FIG. 2. ZD decreased GSH content and GCL expression in IMR-32 cells. IMR-32 cells were incubated for 24 h in control or Zn-deficient (chelated medium containing 1.5μM Zn) media. (A) GCLC, GCLM, and β-tubulin content were measured in total homogenates by Western blot. One representative image is shown. After quantification, results were expressed as the ratio of GCLC or GCLM/β-tubulin. (B) CLC and GCLM mRNA levels were measured by RT-PCR and values normalized to those of the ribosomal protein L32 (RiboL32). (C) GCL activity was measured in IMR-32 cell supernatants as described in Materials and Methods section. Results are shown as means ± SEM of three to four independent experiments. *Significantly different compared with the control group ($p < 0.05$, one-way ANOVA test).

medium was 30% lower than in controls (Fig. 3). Accordingly, Nrf2 protein levels in nuclear fractions from the Zn-deficient IMR-32 cells were significantly lower (28%, $p < 0.01$) than in controls.

ZD Impairs Cellular Defenses Against DA Excess in IMR-32 Cells

High levels of DA cause neuronal oxidative stress as a consequence of the cellular conversion of DA into reactive semiquinone/quinones and the generation of $O_2^{\bullet -}$, H_2O_2, and peroxynitrite. Given that GSH metabolism plays a critical role in protecting cells from DA-induced neuronal injury, we next investigated if ZD affects cellular defense mechanisms against DA-induced oxidative stress. Incubation of IMR-32 in the presence of 50μM DA for 24 h caused a 40% increase in GSH content. In these conditions, DA did not affect cell viability (data not shown). In cells incubated in Zn-deficient medium, DA did not cause a significant increase in GSH levels. In the cells treated with DA, GSH content was 57% lower in the Zn-deficient cells compared with controls (Fig. 4A). GSSG relative levels were higher ($p < 0.001$) in the Zn-deficient cells treated with DA compared with all other groups (1.33 ± 0.20, 1.46 ± 0.27, 0.94 ± 0.16, and 2.50 ± 0.25 GSSG/GSH [%] for the control, control + DA, Zn deficient, and Zn deficient + DA, respectively). In control cells incubated with DA, the raise in GSH levels was coincident with an increase of both *Gclc* and *Gclm* mRNA and protein levels (Figs. 4B and C). Although the percentage of increase was similar in the DA-treated compared with untreated cells for control and Zn-deficient cells, protein and mRNA levels of GCLM and GCLC were 22–36% lower in DA-treated Zn-deficient cells compared with DA-treated controls (Figs. 4B and C). These results indicate that a deficient neuronal Zn status can affect the capacity of cells to respond to DA-induced oxidative stress by upregulating GSH production.

ZD Promotes GCLC Cleavage in IMR-32 Cells

Caspase-3 can cleave the full length GCLC to a 60 kDa peptide (Kojima-Yuasa *et al.*, 2005). In IMR-32 cells incubated in Zn-deficient medium for 24 h, the percentage of 60 kDa peptide relative to total GCLC content was 2.2-fold higher in the Zn-deficient cells compared with controls ($p < 0.001$) (Fig. 5A). Given the different intensity of both bands (full and cleaved GCLC), we had to expose the Western blot membrane to x-ray film for different periods of time to optimize separately the sensitivity for each band. In the representative Western

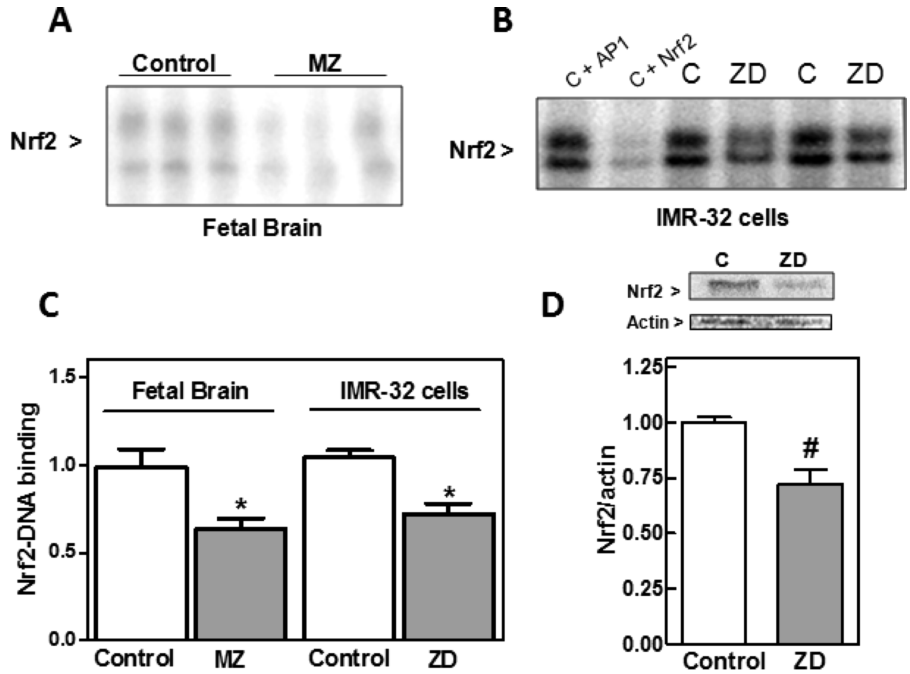

FIG. 3. ZD inhibits Nrf2 nuclear translocation in rat fetal brain and IMR-32 cells. (A) Nrf2-DNA binding measured by EMSA in nuclear fractions isolated from MZD and control GD19 rat fetal brain. One representative EMSA is shown. Results are shown as means ± SEM of five to seven litters for MZD and control groups. (B) Nrf2-DNA binding measured by EMSA in nuclear fractions isolated from IMR-32 cells incubated for 24 h in control (C) or Zn-deficient (chelated medium containing 1.5μM Zn) media. To determine the specificity of the Nrf2-DNA complex, the control nuclear fraction C was incubated in the presence of 100-fold molar excess of unlabeled oligonucleotide containing the consensus sequence for either AP-1 (C + AP-1) or Nrf2 (C + Nrf2) before the binding assay. One representative EMSA out of three independent experiments is shown. (C) After quantification, results are shown as means ± SEM of five to seven litters (fetal brain) and three independent experiments (IMR-32 cells). *Significantly different compared with controls ($p < 0.05$, one-way ANOVA test). (D) Nrf2 and actin content were measured by Western blot in nuclear fractions from cells incubated as described in (B). One representative image is shown. After quantification, results were expressed as the ratio of Nrf2/actin. *,#Significantly different compared with controls (*$p < 0.05$, #$p < 0.01$, one-way ANOVA test).

blot shown in Figure 5A, the 73 kDa (total GCLC) band is overexposed (saturated) in order to show clear differences in the 60 kDa peptide (cleaved GCLC). Ratios were calculated from the optimized exposures, although corrected with samples that showed adequate intensity for the 73 and 60 kDa bands. The increase in GCLC cleavage was prevented when cells were incubated in Zn-deficient media and in the presence of the caspase-3 inhibitor Ac-VEID-CHO (50μM) (Fig. 5A). The content of 60 kDa fragment was markedly higher in Zn-deficient cells incubated with than without DA (Fig. 5A). The observed increase in GCLC cleavage was paralleled by a similar pattern of increase in the cleavage of PARP, a major caspase-3 substrate involved in apoptosis (Fig. 5B, right panel), measured as the ratio of the cleaved (85 kDa) peptide versus the full length protein (116 kDa). The activity of caspase-3 in the Zn-deficient cells incubated with DA was significantly higher than in all other groups after 6 h incubation and remained high up to 24 h (Fig. 5B). After 24 h, caspase-3 activity was 2.9- and 3.7-fold higher in cells incubated in Zn-deficient medium without and with DA, respectively, compared with cells incubated in control medium. Results show that ZD leads to a caspase-3-mediated cleavage of GCLC.

DISCUSSION

Oxidative stress, altered thiol redox status, disregulation of redox signaling, and consequent alterations in the pattern of cell proliferation and apoptosis could in part explain the adverse effects of ZD on brain development (Aimo *et al.*, 2010b; Mackenzie *et al.*, 2007; Uriu-Adams and Keen, 2010). ZD also affects the sensitivity of neuronal cells to oxidant stressors (Aimo and Oteiza, 2006; Mackenzie *et al.*, 2002a). This study presents evidence that a decrease in Zn availability impairs GSH metabolism in human neuroblastoma cells and rat fetal brain. ZD causes a decrease in GSH content that is in part due to a decreased expression of GCL subunits, both at transcriptional and posttranslational levels. Furthermore, Zn-deficient neuronal cells show a decreased capacity to upregulate GSH as part of a protective response against DA-induced toxicity.

GSH is a major cellular antioxidant in the brain (Aimo and Oteiza, 2006; Dringen, 2000). Brain GSH concentration is ~0.4–0.8mM, with higher levels found in astrocytes than in neurons (Bragin *et al.*, 2010). GSH exerts central functions through several mechanisms including: (1) nonenzymatically reacting with superoxide, hydroxyl radical, and nitrogen radicals; (2) as

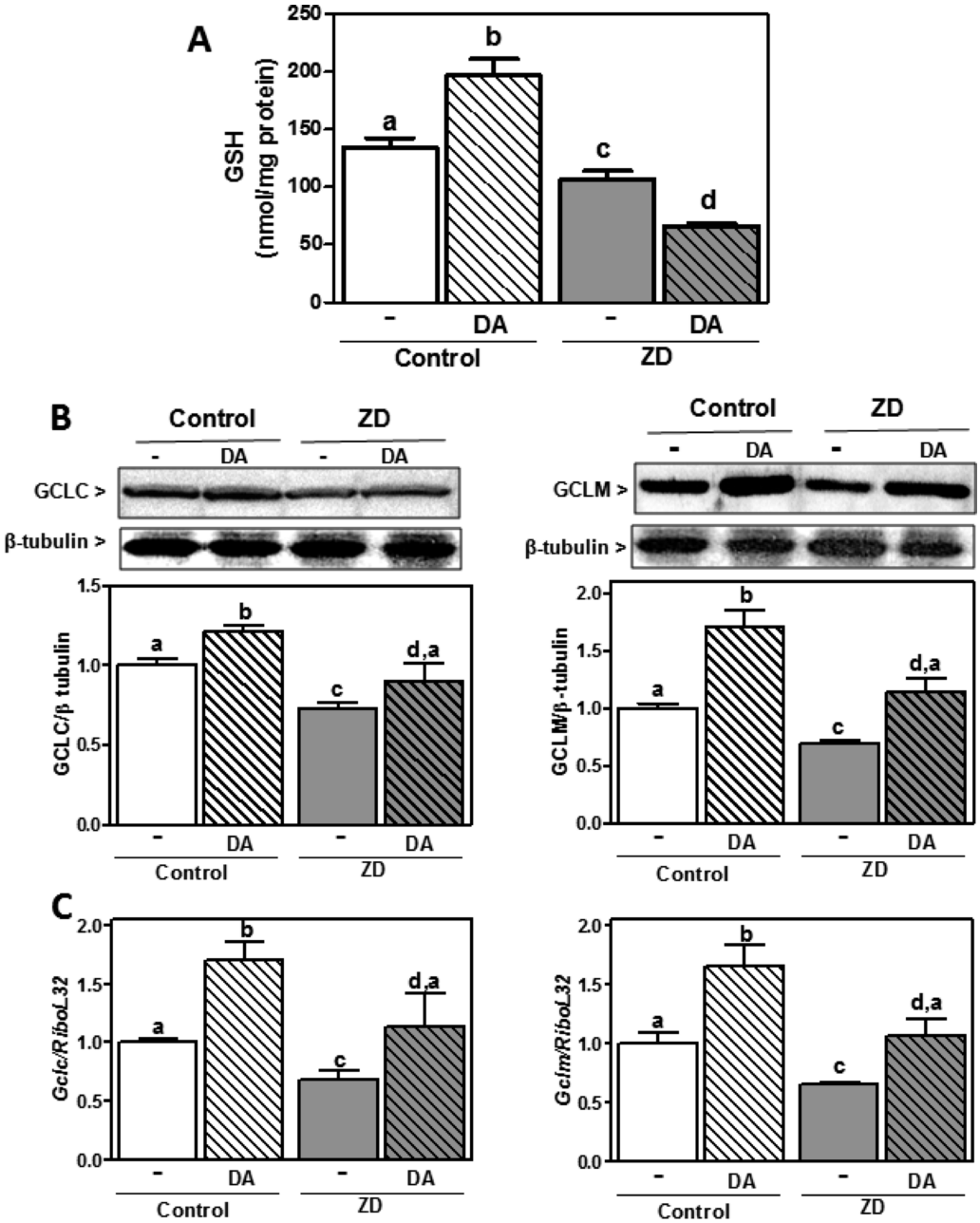

FIG. 4. Effect of DA on GSH content and GCL protein expression in control and Zn-deficient IMR-32 cells. IMR-32 cells were incubated for 24 h in control or Zn-deficient (chelated medium containing 1.5μM Zn) media, in the absence or presence of 50μM DA. (A) GSH concentration in 100,000 × g supernatants. (B) GCLC, GCLM, and β-tubulin content were measured in total homogenates by Western blot. One representative image is shown. After quantification, results were expressed as the ratio of GCLC or GCLM/β-tubulin. (C) GCLC and GCLM mRNA levels were measured by RT-PCR and values normalized to those for the ribosomal protein L32 (RiboL32). Results are shown as means ± SEM of four independent experiments. Values having different letters are significantly different ($p < 0.01$, one-way ANOVA test).

an electron donor for the reduction of H_2O_2 and other peroxides catalyzed by GSH peroxidase; (3) as a carrier/storage form for cysteine; and (4) as the major redox buffer for maintaining intracellular redox homeostasis (Aoyama *et al.*, 2008).

Alterations in GSH metabolism could in part explain ZD-associated neuronal oxidative stress and altered thiol redox status (Aimo *et al.*, 2010a; Mackenzie *et al.*, 2006b; Mackenzie *et al.*, 2011). GSH depletion has been previously observed in different cells and tissues in association with ZD (Kojima-Yuasa *et al.*, 2005; Kraus *et al.*, 1997; Mackenzie *et al.*, 2006b; Oteiza *et al.*, 2001; Tomat *et al.*, 2008). Accordingly, we observed diminished levels of GSH in Zn-deficient fetal brain and IMR-32 human neuroblastoma cells. Neuronal GSH concentration is the resultant of its synthesis, utilization, and export. In

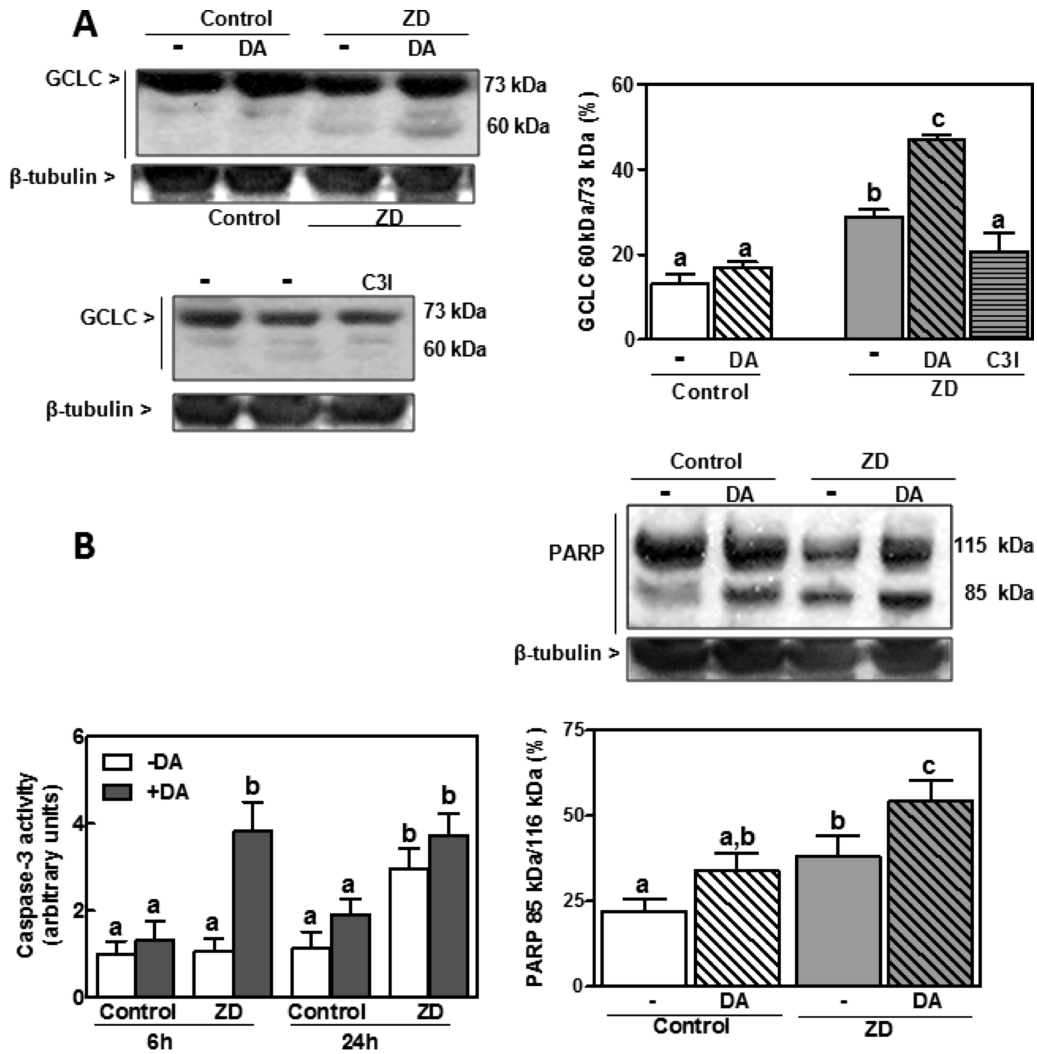

FIG. 5. Effect of DA on GCLC and PARP cleavage and on caspase-3 activity in control and Zn-deficient IMR-32 cells. IMR-32 cells were incubated for 6–24 h in control or Zn-deficient (chelated medium containing 1.5μM Zn) media, in the absence or presence of 50μM DA or 50μM Ac-VEID-CHO (C3I). (A, left panel) Representative Western blot images for full length GCLC (73 kDa), its 60 kDa fragment, and β-tubulin in total cell lysates obtained after 24 h incubation. (Right panel) After quantification, results were expressed as the ratio (%) of 60 kDa/73 kDa GCLC. (B, right panel) Representative Western blot images for full length (116 kDa) and cleaved (85 kDa) PARP and β-tubulin in total cell lysates after 24 h incubation. After quantification, results were expressed as the ratio (%) of 85 kDa/115 kDa PARP. (B, left panel) Caspase-3 activity was measured after 6 and 24 h of incubation as indicated in the Materials and Methods section. Results are shown as means ± SEM of three to five independent experiments. Values having different letters are significantly different ($p < 0.01$, one-way ANOVA test).

Zn-deficient neurons, an increased requirement of GSH can occur as a consequence of the associated increased generation of cellular reactive oxygen and nitrogen species (Mackenzie *et al.*, 2006b; Mackenzie *et al.*, 2011). This is in part due to ZD-triggered activation of the N-methyl-D-aspartate receptor, which leads to calcium influx and to a calcium-mediated activation of NADPH oxidase and nitric oxide synthase (Aimo *et al.*, 2010a). In response to ZD-induced oxidative stress, IMR-32 cells upregulate both copper-Zn and manganese superoxide dismutases, with no changes in GSH peroxidase and reductase activities (Mackenzie *et al.*, 2007).

In terms of GSH synthesis, we observed that ZD impaired the brain/neuronal cell capacity to upregulate components of the GSH synthetic pathway as a protective response to oxidative stress. In Zn-deficient neuronal cells and fetal brain, low GSH levels were coincident with a decreased expression (protein and mRNA levels) of the catalytic and modulatory GCL subunits. The activation of transcription factor (Nrf2), that regulates GCL subunit expression, was also impaired under ZD conditions. Nrf2, a member of the Cap 'n' Collar family of basic leucine zipper proteins, was identified as a key transcription factor for the ARE, a *cis*-regulating DNA sequence located in the promoter region of antioxidant enzymes and phase II detoxifying enzymes (Jones, 2008; Kang *et al.*, 2005). Under basal conditions, Nrf2 is retained in the cytoplasm by Keap1. When the Nrf2/Keap1 complex is disrupted, Nrf2

translocates to the nucleus, binds to DNA, and promotes the transcription of ARE-driven genes, including *Gclc* and *Gclm* (Hansen *et al.* 2004). Zn-sensing sites have been described in Keap1 (McMahon *et al.*, 2010). Zn released from proteins would act as an intracellular second messenger mediating Nrf2/Keap1 sensing of environmental stressors, whereas changes in basal Zn levels are proposed to physiologically modulate Nrf2/Keap1 (McMahon *et al.*, 2010). In line with this, we observed that the decreased GCLC and GCLM expression in both IMR-32 neurons and GD19 fetal brain was coincident with a decreased Nrf2 nuclear translocation and binding to a DNA ARE consensus sequence. Furthermore, ZD decreases NF-κB activation (Mackenzie *et al.*, 2002b), which is also involved in the regulation of GCLC and GCLM transcription. These results suggest that the GSH depletion occurring as a consequence of neuronal ZD can in part occur through an impaired transcriptional GCL regulation.

Disturbances in brain GSH metabolism could contribute to the development of neurodegenerative disorders such as Alzheimer's disease, schizophrenia, and PD (Adams *et al.*, 1991; Gu *et al.*, 1998; Kulak *et al.*, 2012; Raffa *et al.*, 2011). In PD, DA oxidation is proposed to be one mechanism mediating oxidative stress and the loss of dopaminergic neurons. Stressing the relevance of Nrf2 and GSH in the protection of neurons and glial cells against DA toxicity, the upregulation of Nrf2 is neuroprotective in a fly model of PD (Barone *et al.*, 2011), whereas Nrf2 deficits increase DA toxicity *in vivo* and *in vitro* (Jakel *et al.*, 2007). IMR-32 cells responded to DA by increasing GSH levels and GCL subunit expression. In Zn-deficient cells, DA caused an increase in GCLC and GCLM expression, but at a lower extent than those observed in Zn-sufficient cells. GSH levels were not upregulated, whereas GSSG was increased by DA in the Zn-deficient cells. In conditions of oxidative stress, in this case induced by DA, the capacity of GSH reductase to reduce GSSG can be exceeded. Astrocytes and neurons have an ATP-dependent multidrug resistance-associated protein-1 transporter that actively mediates GSSG efflux to prevent a toxic GSSG accumulation inside the cell (Hirrlinger *et al.*, 2002; Minich *et al.*, 2006). GSSG efflux and an impaired capacity to synthesize GSH could explain the low levels of total GSH observed in the Zn-deficient cells exposed to DA.

Results suggest that, as previously observed for lead and iron toxicity (Aimo and Oteiza, 2006; Mackenzie *et al.*, 2002a), ZD increases the susceptibility of neuronal cells to oxidative insults. This higher susceptibility could be in part mediated by an impaired balance of GSH utilization, recycling, and synthesis. Accordingly, a low Zn status impairs nitric oxide-mediated protection of endothelial cells from oxidative stress, in association with altered Nrf2 signaling and decreased GSH levels (Cortese *et al.*, 2008).

It has been previously reported that GCLC is a substrate of caspase-3-mediated cleavage during apoptotic cell death (Aimo and Oteiza, 2006; Franklin *et al.*, 2002). ZD promotes apoptotic cell death, being caspase-3 activation one of the major mechanisms involved (Cortese *et al.*, 2008; Truong-Tran *et al.*, 2001). The protease caspase-3 is a Zn-dependent enzyme, and its activation in ZD has been widely documented in different cells and tissues (Clegg *et al.*, 2005). We observed that both ZD and DA increase caspase-3 activation in IMR-32 cells, with an associated increase of the 60 kDa GCLC cleavage product. This indicates that ZD also affects GCLC at a posttranslational level, which could also impact the capacity of neuronal cells to respond to excess DA. However, the physiological consequence of GCLC cleavage is unclear (Aimo and Oteiza, 2006; Franklin *et al.*, 2002).

Besides an increased susceptibility to oxidative insults, ZD-induced impaired GSH metabolism could have major adverse consequences on brain development. Among them, an imbalance in thiol redox homeostasis can affect protein function and signaling regulation. In fact, we recently observed redox alterations in tubulin thiols in both neuronal cells and GD19 brain (Mackenzie *et al.*, 2011). ZD-associated oxidation of tubulin thiols impairs tubulin polymerization dynamics (Mackenzie *et al.*, 2011), which among other potential consequences, affect the activation of select signaling pathways. In this regard, we observed that microtubules are required for the neuronal nuclear transport of transcription factors NF-κB and nuclear factor of activated T-cells (NFAT), which is markedly affected in Zn-deficient fetal brains and IMR-32 cells (Aimo *et al.*, 2010b; Mackenzie *et al.*, 2006a). Incubation of Zn-deficient cells with compounds (N-acetyl cysteine, α-lipoic acid), which restores cellular GSH levels (Mackenzie *et al.*, 2006b), and tubulin thiol redox state and dynamics (Mackenzie *et al.*, 2011) also re-establishes NF-κB nuclear transport and dependent gene transcription in Zn-deficient IMR-32 cells (Mackenzie *et al.*, 2011).

In summary, this work shows that a decreased Zn availability impairs the GSH synthetic pathway in neuronal cells and fetal brain leading to low GSH brain/neuronal content. Importantly, it demonstrates that this decrease in part occurs as a result of both transcriptional (Nrf2 activation) and post-translational (caspase-3-mediated cleavage) effects on GCL, a central enzyme in GSH synthesis. Findings stress the concept that an impaired capacity to regulate GSH metabolism under conditions of restricted Zn supply could turn neurons more susceptible to pro-oxidant insults like DA.

FUNDING

University of California, Davis; National Institutes of Health (HD 01743).

REFERENCES

Adams, J. D., Jr, Klaidman, L. K., Odunze, I. N., Shen, H. C., and Miller, C. A. (1991). Alzheimer's and Parkinson's disease. Brain levels of glutathione, glutathione disulfide, and vitamin E. *Mol. Chem. Neuropathol.* **14,** 213–226.

Aimo, L., Cherr, G. N., and Oteiza, P. I. (2010a). Low extracellular zinc increases neuronal oxidant production through nadph oxidase and nitric oxide synthase activation. *Free Radic. Biol. Med.* **48,** 1577–1587.

Aimo, L., Mackenzie, G. G., Keenan, A. H., and Oteiza, P. I. (2010b). Gestational zinc deficiency affects the regulation of transcription factors AP-1, NF-κB and NFAT in fetal brain. *J. Nutr. Biochem*. **21,** 1069–1075.

Aimo, L., and Oteiza, P. I. (2006). Zinc deficiency increases the susceptibility of human neuroblastoma cells to lead-induced activator protein-1 activation. *Toxicol. Sci*. **91,** 184–191.

Aoyama, K., Watabe, M., and Nakaki, T. (2008). Regulation of neuronal glutathione synthesis. *J. Pharmacol. Sci*. **108,** 227–238.

Banning, A., and Brigelius-Flohé, R. (2005). NF-kappaB, Nrf2, and HO-1 interplay in redox-regulated VCAM-1 expression. *Antioxid. Redox Signal*. **7,** 889–899.

Barone, M. C., Sykiotis, G. P., and Bohmann, D. (2011). Genetic activation of Nrf2 signaling is sufficient to ameliorate neurodegenerative phenotypes in a Drosophila model of Parkinson's disease. *Dis. Model. Mech*. **4,** 701–707.

Bentley, M. E., Caulfield, L. E., Ram, M., Santizo, M. C., Hurtado, E., Rivera, J. A., Ruel, M. T., and Brown, K. H. (1997). Zinc supplementation affects the activity patterns of rural Guatemalan infants. *J. Nutr*. **127,** 1333–1338.

Bradford, M. M. (1976). A rapid and sensitive method for the quantitation of microgram quantities of protein utilizing the principle of protein-dye binding. *Anal. Biochem*. **72,** 248–254.

Bragin, D. E., Zhou, B., Ramamoorthy, P., Müller, W. S., Connor, J. A., and Shi, H. (2010). Differential changes of glutathione levels in astrocytes and neurons in ischemic brains by two-photon imaging. *J. Cereb. Blood Flow Metab*. **30,** 734–738.

Circu, M. L., and Aw, T. Y. (2010). Reactive oxygen species, cellular redox systems, and apoptosis. *Free Radic. Biol. Med*. **48,** 749–762.

Clegg, M. S., Hanna, L. A., Niles, B. J., Momma, T. Y., and Keen, C. L. (2005). Zinc deficiency-induced cell death. *IUBMB Life* **57,** 661–669.

Cortese, M. M., Suschek, C. V., Wetzel, W., Kröncke, K. D., and Kolb-Bachofen, V. (2008). Zinc protects endothelial cells from hydrogen peroxide via Nrf2-dependent stimulation of glutathione biosynthesis. *Free Radic. Biol. Med*. **44,** 2002–2012.

Dalton, T. P., Dieter, M. Z., Yang, Y., Shertzer, H. G., and Nebert, D. W. (2000). Knockout of the mouse glutamate cysteine ligase catalytic subunit (Gclc) gene: Embryonic lethal when homozygous, and proposed model for moderate glutathione deficiency when heterozygous. *Biochem. Biophys. Res. Commun*. **279,** 324–329.

Dringen, R. (2000). Metabolism and functions of glutathione in brain. *Prog. Neurobiol*. **62,** 649–671.

Duffy, J. Y., Miller, C. M., Rutschilling, G. L., Ridder, G. M., Clegg, M. S., Keen, C. L., and Daston, G. P. (2001). A decrease in intracellular zinc level precedes the detection of early indicators of apoptosis in HL-60 cells. *Apoptosis* **6,** 161–172.

Eibl, J. K., Abdallah, Z., and Ross, G. M. (2010). Zinc-metallothionein: A potential mediator of antioxidant defence mechanisms in response to dopamine-induced stress. *Can. J. Physiol. Pharmacol*. **88,** 305–312.

El-Seweidy, M. M., Hashem, R. M., Abo-El-matty, D. M., and Mohamed, R. H. (2008). Frequent inadequate supply of micronutrients in fast food induces oxidative stress and inflammation in testicular tissues of weanling rats. *J. Pharm. Pharmacol*. **60,** 1237–1242.

Forman, H. J., Zhang, H., and Rinna, A. (2009). Glutathione: Overview of its protective roles, measurement, and biosynthesis. *Mol. Aspects Med*. **30,** 1–12.

Franklin, C. C., Krejsa, C. M., Pierce, R. H., White, C. C., Fausto, N., and Kavanagh, T. J. (2002). Caspase-3-dependent cleavage of the glutamate-L-cysteine ligase catalytic subunit during apoptotic cell death. *Am. J. Pathol*. **160,** 1887–1894.

Frederickson, C. J., Koh, J. Y., and Bush, A. I. (2005). The neurobiology of zinc in health and disease. *Nat. Rev. Neurosci*. **6,** 449–462.

Gardner, J. M., Powell, C. A., Baker-Henningham, H., Walker, S. P., Cole, T. J., and Grantham-McGregor, S. M. (2005). Zinc supplementation and psychosocial stimulation: Effects on the development of undernourished Jamaican children. *Am. J. Clin. Nutr*. **82,** 399–405.

Garrido, M., Tereshchenko, Y., Zhevtsova, Z., Taschenberger, G., Bähr, M., and Kügler, S. (2011). Glutathione depletion and overproduction both initiate degeneration of nigral dopaminergic neurons. *Acta Neuropathol*. **121,** 475–485.

Gu, M., Owen, A. D., Toffa, S. E., Cooper, J. M., Dexter, D. T., Jenner, P., Marsden, C. D., and Schapira, A. H. (1998). Mitochondrial function, GSH and iron in neurodegeneration and Lewy body diseases. *J. Neurol. Sci*. **158,** 24–29.

Gupta, K., Patani, R., Baxter, P., Serio, A., Story, D., Tsujita, T., Hayes, J. D., Pedersen, R. A., Hardingham, G. E., and Chandran, S. (2012). Human embryonic stem cell derived astrocytes mediate non-cell-autonomous neuroprotection through endogenous and drug-induced mechanisms. *Cell Death Differ*. **19,** 779–787.

Gysin, R., Kraftsik, R., Sandell, J., Bovet, P., Chappuis, C., Conus, P., Deppen, P., Preisig, M., Ruiz, V., Steullet, P., *et al.* (2007). Impaired glutathione synthesis in schizophrenia: Convergent genetic and functional evidence. *Proc. Natl Acad. Sci. U.S.A*. **104,** 16621–16626.

Hansen, J. M., Watson, W. H., and Jones, D. P. (2004). Compartmentation of Nrf-2 redox control: Regulation of cytoplasmic activation by glutathione and DNA binding by thioredoxin-1. *Toxicol. Sci*. **82,** 308–317.

Hirrlinger, J., König, J., and Dringen, R. (2002). Expression of mRNAs of multidrug resistance proteins (Mrps) in cultured rat astrocytes, oligodendrocytes, microglial cells and neurones. *J. Neurochem*. **82,** 716–719.

Jakel, R. J., Townsend, J. A., Kraft, A. D., and Johnson, J. A. (2007). Nrf2-mediated protection against 6-hydroxydopamine. *Brain Res*. **1144,** 192–201.

Jia, Z., Zhu, H., Misra, B. R., Li, Y., and Misra, H. P. (2008). Dopamine as a potent inducer of cellular glutathione and NAD(P)H:quinone oxidoreductase 1 in PC12 neuronal cells: A potential adaptive mechanism for dopaminergic neuroprotection. *Neurochem. Res*. **33,** 2197–2205.

Jones, D. P. (2008). Radical-free biology of oxidative stress. *Am. J. Physiol. Cell Physiol*. **295,** C849–C868.

Jones, D. P., Carlson, J. L., Samiec, P. S., Sternberg, P., Jr, Mody, V. C., Jr, Reed, R. L., and Brown, L. A. (1998). Glutathione measurement in human plasma. Evaluation of sample collection, storage and derivatization conditions for analysis of dansyl derivatives by HPLC. *Clin. Chim. Acta* **275,** 175–184.

Kang, K. W., Lee, S. J., and Kim, S. G. (2005). Molecular mechanism of nrf2 activation by oxidative stress. *Antioxid. Redox Signal*. **7,** 1664–1673.

Keen, C. L., Peters, J. M., and Hurley, L. S. (1989). The effect of valproic acid on 65Zn distribution in the pregnant rat. *J. Nutr*. **119,** 607–611.

Kojima-Yuasa, A., Umeda, K., Ohkita, T., Opare Kennedy, D., Nishiguchi, S., and Matsui-Yuasa, I. (2005). Role of reactive oxygen species in zinc deficiency-induced hepatic stellate cell activation. *Free Radic. Biol. Med*. **39,** 631–640.

Kraus, A., Roth, H. P., and Kirchgessner, M. (1997). Supplementation with vitamin C, vitamin E or beta-carotene influences osmotic fragility and oxidative damage of erythrocytes of zinc-deficient rats. *J. Nutr*. **127,** 1290–1296.

Kulak, A., Cuenod, M., and Do, K. Q. (2012). Behavioral phenotyping of glutathione-deficient mice: Relevance to schizophrenia and bipolar disorder. *Behav. Brain Res*. **226,** 563–570.

Kurita, H., Ohsako, S., Hashimoto, S., Yoshinaga, J., and Tohyama, C. (2013). Prenatal zinc deficiency-dependent epigenetic alterations of mouse metallothionein-2 gene. *J. Nutr. Biochem*. **24,** 256–266.

Mackenzie, G. G., Keen, C. L., and Oteiza, P. I. (2002a). Zinc status of human IMR-32 neuroblastoma cells influences their susceptibility to iron-induced oxidative stress. *Dev. Neurosci*. **24,** 125–133.

Mackenzie, G. G., Zago, M. P., Keen, C. L., and Oteiza, P. I. (2002b). Low intracellular zinc impairs the translocation of activated NF-kappa B to the nuclei in human neuroblastoma IMR-32 cells. *J. Biol. Chem*. **277,** 34610–34617.

Mackenzie, G. G., Keen, C. L., and Oteiza, P. I. (2006a). Microtubules are required for NF-kappaB nuclear translocation in neuroblastoma IMR-32 cells: Modulation by zinc. *J. Neurochem*. **99,** 402–415.

Mackenzie, G. G., Zago, M. P., Erlejman, A. G., Aimo, L., Keen, C. L., and Oteiza, P. I. (2006b). alpha-Lipoic acid and N-acetyl cysteine prevent zinc deficiency-induced activation of NF-kappaB and AP-1 transcription factors in human neuroblastoma IMR-32 cells. *Free Radic. Res*. **40,** 75–84.

Mackenzie, G. G., Salvador, G. A., Romero, C., Keen, C. L., and Oteiza, P. I. (2011). A deficit in zinc availability can cause alterations in tubulin thiol redox status in cultured neurons and in the developing fetal rat brain. *Free Radic. Biol. Med*. **51,** 480–489.

Mackenzie, G. G., Zago, M. P., Aimo, L., and Oteiza, P. I. (2007). Zinc deficiency in neuronal biology. *IUBMB Life* **59,** 299–307.

McMahon, M., Lamont, D. J., Beattie, K. A., and Hayes, J. D. (2010). Keap1 perceives stress via three sensors for the endogenous signaling molecules nitric oxide, zinc, and alkenals. *Proc. Natl Acad. Sci. U.S.A*. **107,** 18838–18843.

Minich, T., Riemer, J., Schulz, J. B., Wielinga, P., Wijnholds, J., and Dringen, R. (2006). The multidrug resistance protein 1 (Mrp1), but not Mrp5, mediates export of glutathione and glutathione disulfide from brain astrocytes. *J. Neurochem*. **97,** 373–384.

Osborn, L., Kunkel, S., and Nabel, G. J. (1989). Tumor necrosis factor alpha and interleukin 1 stimulate the human immunodeficiency virus enhancer by activation of the nuclear factor kappa B. *Proc. Natl Acad. Sci. U.S.A*. **86,** 2336–2340.

Oteiza, P. I., Clegg, M. S., and Keen, C. L. (2001). Short-term zinc deficiency affects nuclear factor-kappab nuclear binding activity in rat testes. *J. Nutr*. **131,** 21–26.

Oteiza, P. I., Clegg, M. S., Zago, M. P., and Keen, C. L. (2000). Zinc deficiency induces oxidative stress and AP-1 activation in 3T3 cells. *Free Radic. Biol. Med*. **28,** 1091–1099.

Oteiza, P. I., and Mackenzie, G. G. (2005). Zinc, oxidant-triggered cell signaling, and human health. *Mol. Aspects Med*. **26,** 245–255.

Penland, J. G., Sandstead, H. H., Alcock, N. W., Dayal, H. H., Chen, X. C., Li, J. S., Zhao, F., and Yang, J. J. (1997). A preliminary report: Effects of zinc and micronutrient repletion on growth and neuropsychological function of urban Chinese children. *J. Am. Coll. Nutr*. **16,** 268–272.

Raffa, M., Atig, F., Mhalla, A., Kerkeni, A., and Mechri, A. (2011). Decreased glutathione levels and impaired antioxidant enzyme activities in drug-naive first-episode schizophrenic patients. *BMC Psychiatry* **11,** 124.

Soto-Otero, R., Méndez-Alvarez, E., Hermida-Ameijeiras, A., Muñoz-Patiño, A. M., and Labandeira-Garcia, J. L. (2000). Autoxidation and neurotoxicity of 6-hydroxydopamine in the presence of some antioxidants: Potential implication in relation to the pathogenesis of Parkinson's disease. *J. Neurochem*. **74,** 1605–1612.

Tomat, A. L., Inserra, F., Veiras, L., Vallone, M. C., Balaszczuk, A. M., Costa, M. A., and Arranz, C. (2008). Moderate zinc restriction during fetal and postnatal growth of rats: Effects on adult arterial blood pressure and kidney. *Am. J. Physiol. Regul. Integr. Comp. Physiol*. **295,** R543–R549.

Truong-Tran, A. Q., Carter, J., Ruffin, R. E., and Zalewski, P. D. (2001). The role of zinc in caspase activation and apoptotic cell death. *Biometals* **14,** 315–330.

Uriu-Adams, J. Y., and Keen, C. L. (2010). Zinc and reproduction: Effects of zinc deficiency on prenatal and early postnatal development. *Birth Defects Res. B Dev. Reprod. Toxicol*. **89,** 313–325.

White, C. C., Viernes, H., Krejsa, C. M., Botta, D., and Kavanagh, T. J. (2003). Fluorescence-based microtiter plate assay for glutamate-cysteine ligase activity. *Anal. Biochem*. **318,** 175–180.